

# Development of an oscillating magnetic field-assisted supercooling system for bovine embryo preservation

Jun Hwi So<sup>1#</sup>, Byung Hyun Ju<sup>2,3#</sup>, Sung Yong Joe<sup>4</sup>, Youngbok Ko<sup>5,6</sup>,  
Soojin Jun<sup>7</sup>, Min Kyu Kim<sup>2,3#\*</sup>, Seung Hyun Lee<sup>1,4,6#\*</sup>

<sup>1</sup>Department of Smart Agriculture Systems, Chungnam National University, Daejeon, Korea

<sup>2</sup>Division of Animal and Dairy Science, Chungnam National University, Daejeon, Korea

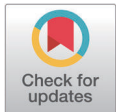
<sup>3</sup>MK Biotech Inc., Daejeon, Korea

<sup>4</sup>Department of Smart Agriculture Systems Machinery Engineering, Chungnam National University, Daejeon, Korea

<sup>5</sup>Department of Obstetrics and Gynecology, Chungnam National University, Daejeon, Korea

<sup>6</sup>Neo Vitalink Inc., Daejeon, Korea

<sup>7</sup>Department of Human Nutrition, Food, and Animal Sciences, University of Hawaii, Honolulu, HI, USA



Received: Nov 28, 2025

Revised: Jan 7, 2026

Accepted: Jan 21, 2026

#These authors contributed equally to this work.

## \*Corresponding author

Min Kyu Kim

E-mail: [kminkyu@cnu.ac.kr](mailto:kminkyu@cnu.ac.kr)

Seung Hyun Lee

E-mail: [seunglee2@cnu.ac.kr](mailto:seunglee2@cnu.ac.kr)

Copyright © 2026 Korean Society of Animal Science and Technology. This is an Open Access article distributed under the terms of the Creative Commons Attribution Non-Commercial License (<http://creativecommons.org/licenses/by-nc/4.0/>) which permits unrestricted non-commercial use, distribution, and reproduction in any medium, provided the original work is properly cited.

## ORCID

Jun Hwi So

<https://orcid.org/0000-0001-9479-6000>

Byung Hyun Ju

<https://orcid.org/0000-0003-1672-4604>

Sung Yong Joe

<https://orcid.org/0000-0002-8482-9777>

Youngbok Ko

<https://orcid.org/0000-0002-8972-6742>

Soojin Jun

<https://orcid.org/0000-0002-0865-4565>

Min Kyu Kim

<https://orcid.org/0000-0002-9259-8219>

## Abstract

*In-vitro*-produced embryos have become an important biomaterial for accelerating genetic improvements in livestock, increasing the need for reliable short- and mid-term preservation strategies. This study was conducted to investigate the effects of oscillating-magnetic-field-assisted supercooling on the survival of bovine *in vitro* fertilization embryos. A supercooling preservation system combining Helmholtz-type coils with a precise circulating cooling chamber was designed and fabricated to maintain the embryos in a uniform supercooled state. Blastocyst-stage embryos were preserved at  $-4^{\circ}\text{C}$  in a hypothermic preservation medium under exposure to an oscillating magnetic field of 10 Hz with flux densities ranging from 0 to 20 mT. The preservation medium remained stably supercooled at  $-4^{\circ}\text{C}$  without freezing under all magnetic field conditions, and the magnetic flux density did not alter the cooling behavior. The embryos were preserved for 24 h and subsequently cultured for an additional 24 h to assess their post-preservation viability. Survival rates were higher in all magnetic field groups than in the control group (0 mT), with values of 48.66% (0 mT), 60.07% (5 mT), 62.85% (10 mT), 75.69% (15 mT), and 68.96% (20 mT). Notably, the 15 mT group exhibited the highest survival rate, showing a significant improvement over the control. Although the magnetic field did not affect the supercooling characteristics of the preservation solution, it markedly enhanced embryo survival at  $-4^{\circ}\text{C}$ . The results demonstrated that the application of an oscillating magnetic field did not disrupt the stability of the supercooled state while also improving cellular tolerance to low-temperature stress. These findings provide a promising foundation on which to develop magnetic-field-based non-freezing preservation technologies for biological specimens.

**Keywords:** Embryo, Supercooling, Oscillating magnetic field, Temperature control, Viability

Seung Hyun Lee  
<https://orcid.org/0000-0002-2096-3053>

#### Competing interests

No potential conflict of interest relevant to this article was reported.

#### Funding sources

This research was funded by Chungnam National University, grant number 2024-0899-01.

#### Acknowledgements

Not applicable.

#### Availability of data and material

Upon reasonable request, the datasets of this study can be available from the corresponding author.

#### Authors' contributions

Conceptualization: Kim MK, Lee SH.  
 Data curation: So JH, Ju BH, Kim MK, Lee SH.  
 Formal analysis: So JH, Ju BH, Ko Y.  
 Methodology: So JH, Ju BH, Joe SY, Jun SJ.  
 Software: So JH, Ju BH.  
 Validation: So JH, Ju BH.  
 Investigation: So JH, Ju BH.  
 Writing - original draft: So JH, Ju BH.  
 Writing - review & editing: So JH, Ju BH, Joe SY, Ko Y, Jun S, Kim MK, Lee SH.

#### Ethics approval and consent to participate

The use of bovine ovaries in this study was reviewed and approved by the Institutional Animal Care and Use Committee of Chungnam National University (IACUC Approval No. 202103A-CNU-002).

#### Declaration of generative AI

No AI tools were used in this article.

## INTRODUCTION

Embryos constitute the earliest stage of life and mark the onset of the reproductive process. Since the technological advancements in *in vitro* fertilization (IVF) during the 1990s, the reliable *in vitro* production of high-quality embryos has become feasible [1]. As a result, embryos have gained increasing importance as a biological resource for enhancing genetic dissemination and reproductive efficiency. In this context, embryo preservation has progressed beyond simple storage toward more advanced strategies aimed at maintaining viability for extended periods, thereby underscoring the growing need for stable preservation and management systems, particularly in livestock production [2].

Embryo preservation methods are generally classified according to the storage duration into hypothermic preservation (2 °C–8 °C) for short-term storage and cryopreservation (–196 °C) for long-term storage. Slow freezing and vitrification are widely used in cryopreservation and allow cells to be stored for long periods or even virtually indefinitely. However, a major limitation of cryopreservation is the cellular damage caused by osmotic imbalances and the formation of ice crystals during the freezing process [3]. Although vitrification has demonstrated improved preservation outcomes in recent studies, it still requires high concentrations of cryoprotectants and considerable technical expertise, making it unsuitable for short- and medium-term preservation [3,4]. On the other hand, hypothermic preservation requires only simple equipment and handling procedures to extend the lifespan by suppressing cellular metabolic activity. However, this method is inherently limited to very short-term preservation, as survival declines rapidly due to membrane damage, ionic imbalances, and the accumulation of reactive oxygen species [5]. To overcome these limitations, the substantial efforts have focused on alternative strategies, including optimization of the cryoprotectant composition [6,7], controlled ice nucleation [8], high-pressure freezing [9], and supercooling [10].

Among these preservation technologies, supercooling, capable of maintaining liquid products below their freezing points without the formation of ice crystals, has been proposed as an alternative non-freezing preservation method that minimizes cryoinjuries in cells and tissues [11,12]. However, because the supercooled state is thermodynamically metastable, even minor perturbations such as mechanical vibrations, impurities, interfacial heterogeneities, or irregularities on container surfaces can readily induce ice nucleation [13]. Therefore, precise control of the physical conditions is essential to maintain a stable supercooled state.

Recent studies have explored the use of magnetic fields to suppress ice nucleation and stabilize the supercooled state [14]. Previous studies indicated that magnetic fields can modulate the orientation of water molecules and the organization of hydrogen-bond networks, thereby lowering the freezing onset temperature and slowing ice-crystal growth [15]. In particular, oscillating magnetic field (OMF), in which the magnetic polarity periodically reverses, has been shown to inhibit ice crystallization within agricultural and biological materials [16,17]. Magnetic-field-assisted supercooling preservation has been investigated primarily in relation to agricultural products, whereas studies involving embryos are still extremely limited.

The objective of the present study was to develop an OMF-assisted supercooling preservation system based on the aforementioned physical principles. The system consists of a temperature-controlled chamber integrated with a magnetic field generator to maintain embryos under stable thermal conditions while applying periodic magnetic field oscillations. To evaluate the system performance, we evaluated the supercooling stability and operational characteristics and assessed embryo survival after preservation at –4 °C under magnetic flux densities of 0–20 mT as a biological validation metric. Through these evaluations, this study demonstrates the feasibility of a magnetic-field-based supercooling platform for short- and medium-term embryo preservation.

## MATERIALS AND METHODS

### Sample preparation

Bovine embryos were supplied by MK Biotech using an IVF protocol. The embryos used in this study were produced as described in a previous study [18] and were all at the blastocyst stage. Only morphologically normal embryos that met the quality criteria were selected for the experiment. Within each independent experimental run, embryos derived from multiple donor cows (3–6 donors per batch) were pooled prior to random allocation such that embryos from each donor were distributed across all treatment groups, minimizing donor-specific bias.

The preservation solution used for the supercooling experiments was formulated by MK Biotech based on the composition described in earlier work [6], which employed a tissue culture medium 199 (TCM 199; Gibco) supplemented with fetal bovine serum (FBS; Gibco) and HEPES (Sigma-Aldrich). Each embryo was individually placed in a 1.2 mL tube containing the preservation solution, with 6–9 embryos per group. Samples were transported in insulated containers with ice packs and were used for the experiments immediately upon arrival.

### Experimental system configuration

The overall configuration of the supercooling and OMF system used in this study is shown in Fig. 1A. The system consisted of a custom-built Helmholtz coil, a cooling chamber for embryo preservation, a circulating chiller (LC-LT412, LKLAB Korea), and a custom-built programmable pulse power supply. The power supply was designed to generate an alternating pulsed waveform with adjustable voltages (from 1 V to 200 V), on/off duty cycles (from 10% to 90%), and frequencies (from 1 Hz to 20 kHz). The voltage and current applied to the Helmholtz coil were continuously monitored and recorded in real time using a differential probe (PR-60, B&K Precision), a current monitor (Model 150, Pearson Electronics) and an oscilloscope (TBS1102B, Tektronix). In this study, bipolar square-pulse voltage with a 50% duty cycle and 10 Hz frequency was applied to the coils to generate the OMF.

As shown in Fig. 1B, the Helmholtz coil pair was symmetrically positioned within the cooling chamber to generate a uniform magnetic field throughout the chamber interior. The coil bobbins were spaced apart from the chamber wall to minimize thermal and mechanical interference, and coil heating was controlled using surface heat sinks combined with forced-air cooling fans (Fig. 1C). All experiments were conducted under laboratory ambient conditions ( $\leq 25^\circ\text{C}$ ), and a PID control system was employed to maintain the internal chamber temperature independent of ambient temperatures or heat generation by the coil.

### Cooling chamber design

The cooling system was designed and manufactured to maintain a uniform temperature inside the chamber and to withstand the thermal load associated with coolant circulation (Fig. 2A). The main body of the chamber consisted of a high-strength acrylic material with excellent thermal insulation properties and incorporated a double-wall structure for enhanced stability. The samples were mounted on a three-tier rack installed inside the chamber, with four sample tubes placed on each level, allowing a total of twelve samples to be accommodated simultaneously.

A propylene-glycol-based coolant (Antifreeze  $-60^\circ\text{F}$ , Star Brite) was circulated within the system, with the coolant flow rate set to 3 L/min. The inlet and outlet were positioned at the upper and lower sections of the chamber, respectively, to establish a stable convective flow. The chamber opening was sealed with an acrylic cover and polyethylene foam insulation to minimize heat loss. The chamber temperature was maintained at  $-4 \pm 0.2^\circ\text{C}$ .

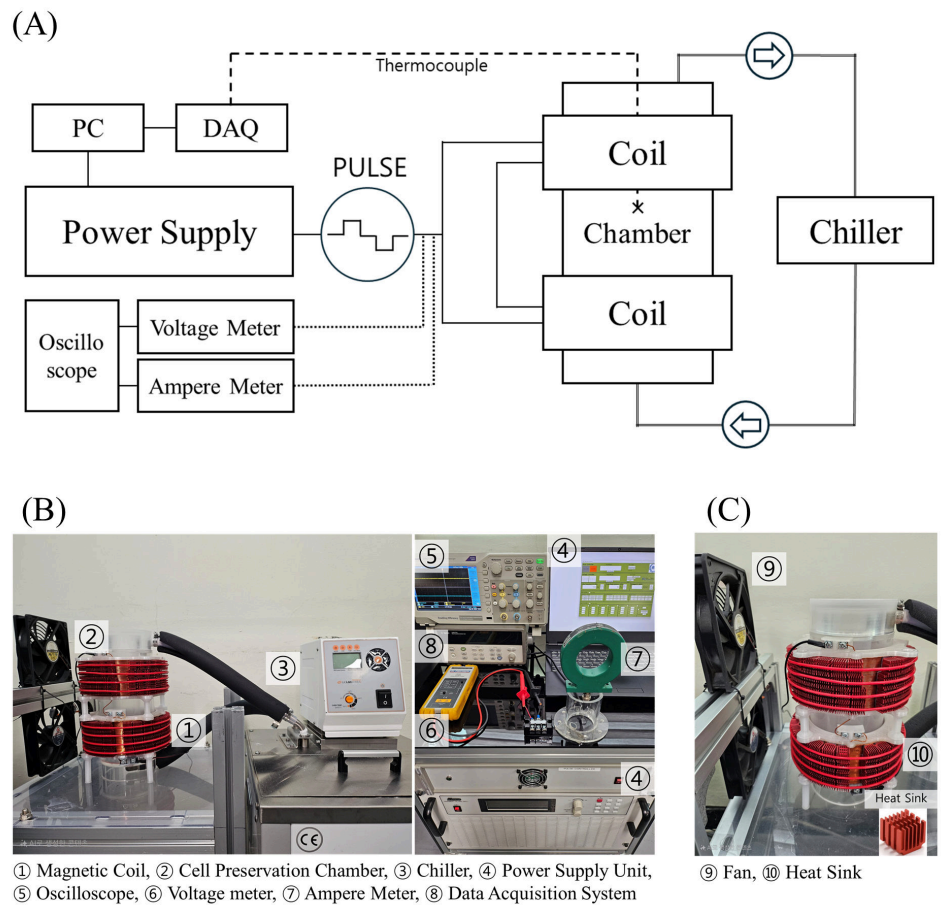


**Fig. 1.** Design of the oscillating-magnetic-field (OMF)-assisted supercooling system. (A) Schematic diagram of the system. (B) Overall system assembly with a Helmholtz coil and a control unit. (C) Heat-dissipation structure showing heat sinks and the airflow design. PC, personal computer; DAQ, data acquisition system.

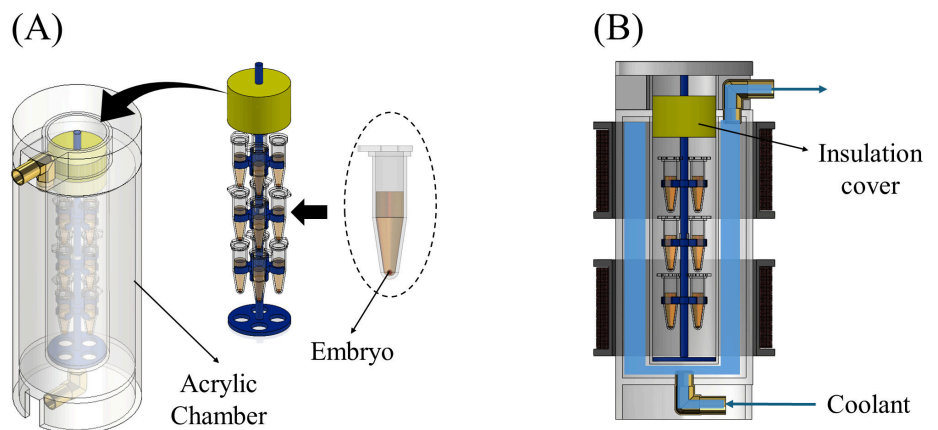


**Fig. 2.** Structure of the embryo preservation chamber. (A) Double-wall acrylic chamber with a three-tier rack holding twelve sample tubes (four per layer). (B) Cooling mechanism showing the flow of propylene-glycol coolant between the inner and outer walls.

### Helmholtz coil assembly

A Helmholtz configuration, consisting of two identical circular coils positioned at a fixed distance, was adopted to generate a uniform magnetic field (Fig. 3A). The magnetic flux density distribution was analyzed using COMSOL Multiphysics v.6.2 (COMSOL AB) based on a direct current (DC) magnetic field model for simplicity and to approximate quasi-static field conditions, as described in a previous study [19]. The coils were wound with copper wire with a diameter of 1 mm, comprising 490 turns per coil. Non-magnetic materials such as air, plastic, the coolant, and the biological samples were neglected in the magnetic simulation (Fig. 3B).

The simulation results were used to evaluate the magnetic field distribution and to determine the optimal sample placement region. After defining the placement positions, alternating voltage was applied to the coils, with the input voltage adjusted to achieve a magnetic flux density of 15 mT at the designated sample locations.

### Temperature profile measurements

The internal temperature of the cooling chamber was measured and recorded in all experiments. All temperatures were measured using T-type thermocouple (TT-T-36-SLE, Omega Engineering) that minimizes magnetization effects in the magnetic field environment. The T-type thermocouple, composed of non-magnetic Cu-Constantan materials, is also known to exhibit minimal interference under magnetic fields [20]. For the solution-level supercooling experiments, the thermocouple was attached to the outer surface of the sample tube. For the embryo preservation experiments, the thermocouple was attached to the sample holder and positioned at the geometric center of the cooling chamber to monitor the chamber air temperature. The thermocouples were connected to a data acquisition unit (34970A, Keysight Technologies) to record temperature data at 5 s intervals.

### Measurement of supercooling characteristics in solutions

The effects of the OMFs on the cooling behavior of the embryo preservation solution were analyzed in this study. Each sample (1.2 mL) was placed inside the cooling chamber, and the magnetic field

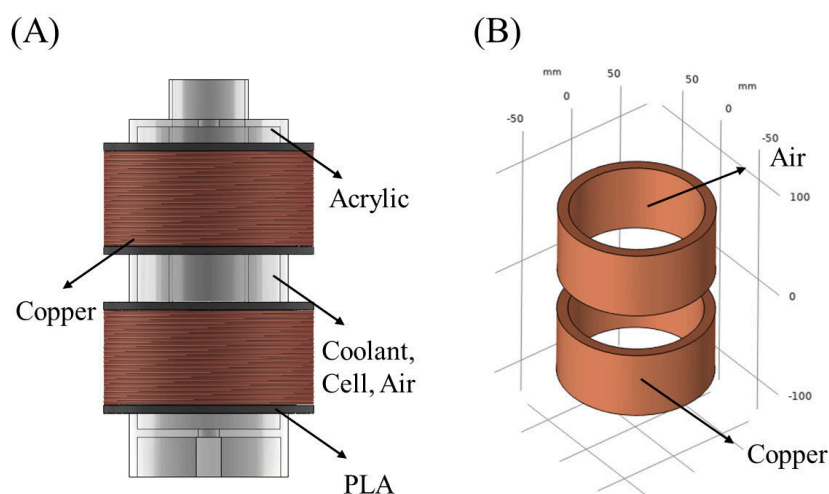


**Fig. 3. Geometry of the Helmholtz coil.** (A) Design drawing of the Helmholtz coil showing two identical circular coils arranged with a spacing equal to the coil radius. (B) 3D simulation geometry constructed in COMSOL Multiphysics, representing the model used for the magnetic field calculation. The coordinate axes are expressed in millimeters (mm).

was applied when the temperature inside cooling chamber reached  $-4^{\circ}\text{C}$ . A preservation temperature of  $-4^{\circ}\text{C}$  was selected based on experimental design considerations and consistency with commonly adopted conditions in supercooling-based embryo preservation studies. This temperature was chosen to enable stable maintenance of the supercooled state during short-term preservation while remaining compatible with embryo viability. The magnetic field strength levels were set to 0 (control), 5, 10, and 15 mT. OMFs with a fixed frequency of 10 Hz were applied to all experimental groups. During the cooling process, the temperature was continuously recorded in real time until the solution temperature stabilized at  $-4^{\circ}\text{C}$ .

Each sample consisted of 1.2 mL of preservation solution contained in a cell storage tube, and each was introduced into the cooling chamber to analyze temporal variations in the temperature. Three samples were used per magnetic field condition, and all experiments were repeated three times to ensure reproducibility. After reaching  $-4^{\circ}\text{C}$ , the samples were maintained at this temperature for 30 min. Successful maintenance of the supercooled state was defined by the absence of visible ice formation and abrupt temperature increases indicative of latent heat release associated with ice nucleation.

### Embryo supercooling preservation procedure

Embryo supercooling preservation experiments were conducted to evaluate the effects of the supercooled state on embryo survival (Fig. 4). All experiments were performed in the cooling chamber maintained at  $-4^{\circ}\text{C}$ , with magnetic flux densities of 0 mT (control), 5 mT, 10 mT, 15 mT, and 20 mT applied. Solution-level experiments were limited to magnetic flux densities in a range of 0–15 mT based on preliminary design considerations indicating that this range was sufficient to evaluate solution-level supercooling stability, whereas the embryo preservation experiments included 20 mT to assess system performance at the upper operational limit of the magnetic field generator. Prior to sample loading, the cooling system and magnetic field generator were pre-activated to ensure thermal

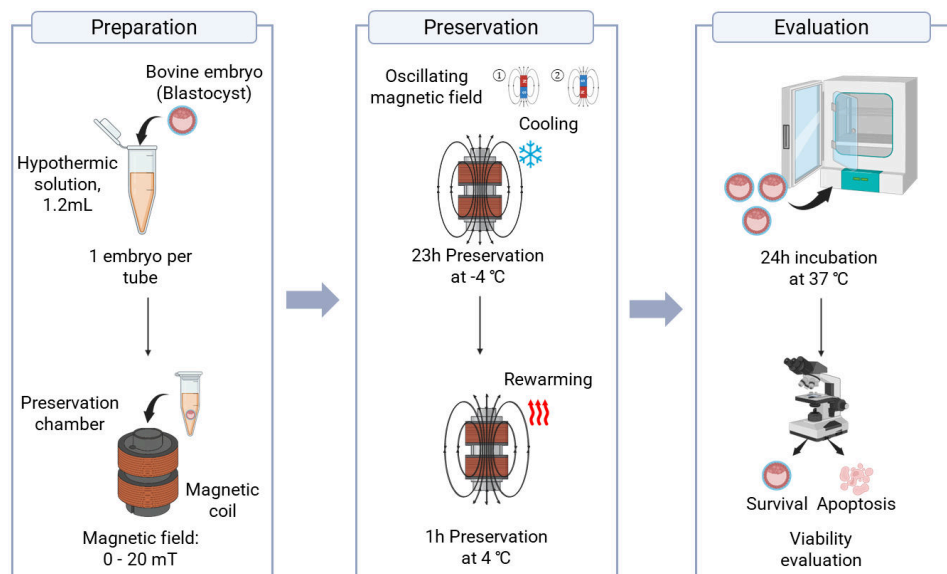


**Fig. 4. Experimental workflow of the oscillating-magnetic-field-assisted supercooling procedure for bovine embryos.** The process consists of three main stages. (1) Preparation — a single *in vitro* fertilization (IVF)-derived bovine blastocyst was placed in a 1.2 mL tube containing a preservation solution; (2) Preservation — samples were stored at  $-4^{\circ}\text{C}$  under oscillating magnetic fields (0–20 mT) for 23 h, followed by 1 h of warming at  $4^{\circ}\text{C}$ ; (3) Post-preservation evaluation — embryos were incubated at  $38.5^{\circ}\text{C}$  for 24 h, and viability was assessed based on survival and apoptosis outcomes.

and magnetic stabilization inside the chamber.

After stabilization, the embryo samples were introduced into the chamber and preserved at  $-4^{\circ}\text{C}$  for 23 hours. Subsequently, the chamber temperature was gradually increased to  $4^{\circ}\text{C}$  over a one-hour rewarming step. The total preservation time was 24 hours, after which all samples were immediately transferred to a modified CR2 medium containing 5% FBS and incubated at  $38.5^{\circ}\text{C}$  under 5%  $\text{CO}_2$  for 24 hours, based on culture conditions described previously [18].

### Viability assessment of preserved embryos

After the 24-hour preservation process, the embryos were transferred to an incubator and cultured for an additional 24 hours. The viability of each embryo was evaluated under a stereomicroscope based on morphological integrity. The survival rate was calculated as follows:

$$\text{Survival rate (\%)} = \left( \frac{\text{Number of viable embryos}}{\text{Total number of embryos}} \right) \times 100$$

### Statistical analysis

All experiments were independently repeated at least three times. Statistical analyses were conducted using SPSS Statistics v.19.0 (IBM). The mean survival rate from each independent trial was used to analyze differences among groups. Data normality and homogeneity of variance were verified using the Shapiro-Wilk test and Levene's test, respectively. One-way analysis of variance (ANOVA) was conducted, and Bonferroni correction was applied for multiple comparisons when significant differences were detected. Differences were considered statistically significant at  $p < 0.05$ .

## RESULTS

### System performance validation

#### Temperature uniformity in the cooling chamber

The temperature uniformity inside the cooling chamber was secured to ensure a stable cooling environment during embryo preservation. As shown in Fig. 5, the temperature was recorded along both the vertical and horizontal directions. For the vertical measurement, sample tubes were placed at three levels (upper, middle, and lower), while for the horizontal measurement, four points were arranged in a circular pattern on the same level to evaluate any temperature variations.

As summarized in Table 1, the reported temperature values represent deviations from the target

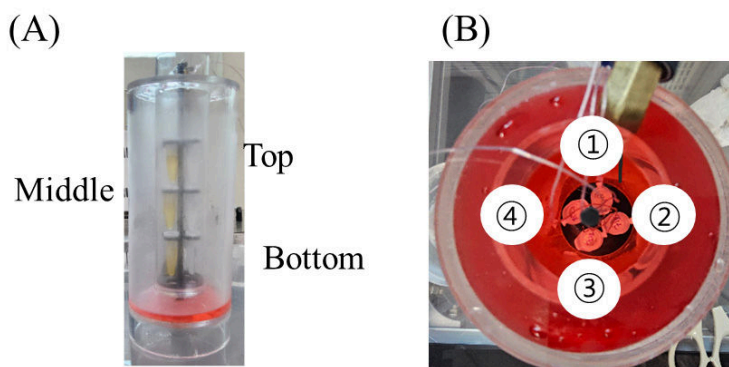


**Fig. 5.** Temperature measurement point inside the cooling chamber. (A) Vertical and (B) Horizontal.

**Table 1.** Temperature deviation relative to reference points within the chamber

Measurement region	Temperature point	Temperature difference relative to reference point (°C) <sup>1)</sup>			
		Mean	SD	Min	Max
Vertical distribution	Top	0.05	± 0.02	-0.02	0.14
	Middle			Ref <sup>2)</sup>	
	Bottom	-0.04	± 0.02	-0.11	0.02
Horizontal distribution at middle plane	①			Ref <sup>3)</sup>	
	②	-0.006	± 0.018	-0.08	0.06
	③	0.006	± 0.02	-0.07	0.09
	④	0.015	± 0.023	-0.07	0.10

<sup>1)</sup>Positive (+) values indicate temperatures higher than the reference, whereas negative (-) values indicate temperatures lower than the reference.

<sup>2)</sup>For vertical distribution, the middle position was used as the reference.

<sup>3)</sup>For horizontal distribution, point ① at the middle plane was used as the reference.

chamber temperature of  $-4^{\circ}\text{C}$ . The average temperature deviations of the upper and lower levels were within  $\pm 0.05^{\circ}\text{C}$  relative to the middle level, with maximum deviations of  $0.14^{\circ}\text{C}$  at the top and  $0.02^{\circ}\text{C}$  at the bottom. Within each level, the average temperature difference among the four measurement points was less than  $0.015^{\circ}\text{C}$ , with maximum deviation of  $0.1^{\circ}\text{C}$ . Overall, the cooling chamber maintained a stable thermal environment centered at  $-4^{\circ}\text{C}$ , with vertical and horizontal temperature uniformity within  $\pm 0.5^{\circ}\text{C}$  and  $\pm 0.2^{\circ}\text{C}$ , respectively.

### **Magnetic flux distribution of the Helmholtz coils**

The magnetic coils served as a key component for generating a uniform magnetic field within the embryo preservation chamber. The magnetic flux distribution of the fabricated Helmholtz coils was validated through both simulation and experimental measurements (Fig. 6). As shown in Fig. 6A, the designed Helmholtz configuration produced a typical magnetic field-line pattern characteristic of this geometry. The coils generated an axial magnetic field whose strength and direction were linearly proportional to the magnitude and polarity of the applied current.

When square-pulsed alternating current was applied to the coils, the magnetic field direction was periodically reversed, forming an OMF, as confirmed by experimental measurements (Fig. 6B). Under experimental operating conditions, stable OMF generation was achievable up to a magnetic flux density of 20 mT (data not shown). At higher magnetic field strength settings, heat generated in the coils could not be sufficiently dissipated, preventing stable operation. Based on magnetic field simulations, a uniform magnetic field region corresponding to  $\pm 5\%$  of the target magnetic flux density (15 mT) was identified along the central axis of the coil ( $y = 0$  mm; Fig. 6C). This uniform region comprised three axial segments ( $-63$  to  $-49$  mm,  $-32$  to  $-9$  mm, and  $9$  to  $32$  mm). Accordingly, the sample positions were set to  $-60$ ,  $-20$ , and  $+20$  mm, each of which was located within the identified uniform-field region.

While the simulation predicted a magnetic flux density of 15 mT at 3.1 A, the experimental measurement confirmed that 15 mT was achieved at a 3.2 A peak under alternating current excitation (Fig. 6D).

### **Effects of the magnetic field on the cooling characteristics of the solutions**

The effects of different OMFs on the cooling behavior of the preservation solution were analyzed (Fig. 7). A differential scanning calorimetry (DSC) analysis revealed that the freezing point of the preservation solution was  $-1.4^{\circ}\text{C}$  (Fig. 7A). Subsequently, temperature changes were monitored in

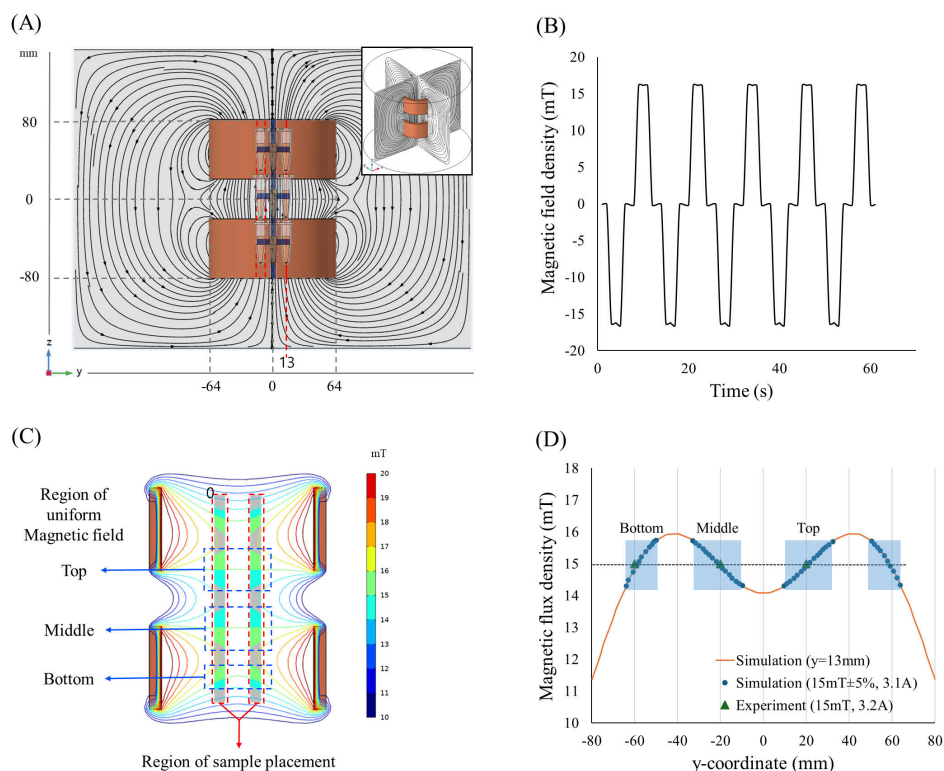


**Fig. 6. Magnetic flux density distribution of the Helmholtz coil.** (A) simulated magnetic field lines of the Helmholtz configuration, (B) oscillating magnetic field generated by a bipolar pulse voltage, (C) axial magnetic flux distribution obtained from the simulation, and (D) comparison between simulated and experimentally measured magnetic flux densities along the y-axis, showing that both results agree within  $\pm 5\%$  around the target field strength (15 mT).

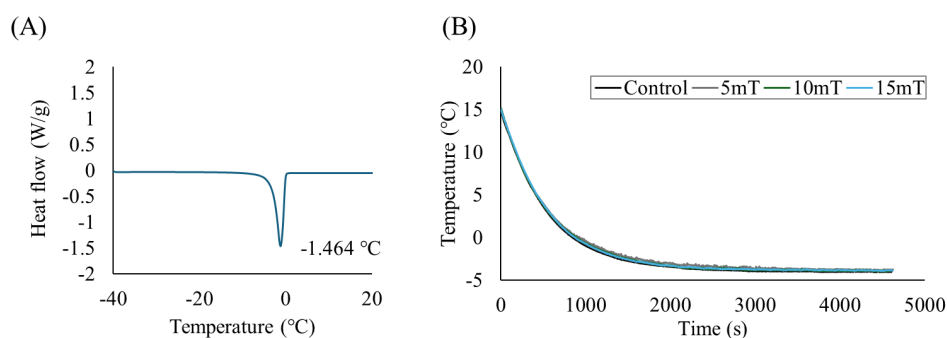


**Fig. 7. Cooling behavior of the preservation solution under oscillating magnetic field conditions.** (A) The differential scanning calorimetry (DSC) analysis revealed a freezing point at  $-1.4^{\circ}\text{C}$ . (B) The temperature profiles obtained under a magnetic field intensity range of 0–15 mT exhibited nearly identical cooling curves.

real time for the same solution placed in a cooling chamber maintained at  $-4^{\circ}\text{C}$  under magnetic flux densities of 0 mT, 5 mT, 10 mT, and 15 mT.

After reaching  $-4^{\circ}\text{C}$ , all samples were maintained at this temperature for a 30 min observation period. Under all magnetic field conditions, the solution samples remained unfrozen and maintained a stable supercooled state, as evidenced by the absence of visible ice formation and the absence of abrupt temperature increases associated with latent heat release. The temperature

**Table 2.** Frequency of the supercooled preservation solution

Magnetic flux density (mT)	No. of sample	No. of Supercooled
0 (Control)	9	9
5	9	9
10	9	9
15	9	9

profiles exhibited nearly identical patterns regardless of the magnetic field intensity (Fig. 7B). As summarized in Table 2, all nine samples under each magnetic field condition successfully remained in the supercooled state throughout the observation period.

### Effects of the magnetic field on embryo preservation

Embryo viability was evaluated after 24 hours of preservation under supercooled conditions at  $-4^{\circ}\text{C}$ . Fig. 8A shows the internal temperature of the cooling chamber during embryo preservation. In the temperature profile, oscillations were observed in the thermocouple readings due to magnetic field interference; however, these fluctuations did not affect the actual internal temperature, and the chamber temperature remained stable around  $-4^{\circ}\text{C}$  throughout the experimental period. Fig. 8B presents representative images of embryos observed after post-preservation culturing. The embryos were classified as survived, degenerated, or hatched based on their morphology. Table 3 summarizes the average survival rates of embryos preserved under different magnetic flux densities. The control group (0 mT) showed a mean survival rate of  $48.66\% \pm 7.07\%$ , while slightly higher survival rates were observed at 5 mT ( $60.07\% \pm 5.48\%$ ) and 10 mT ( $62.85\% \pm 5.24\%$ ), although these differences were not statistically significant. In contrast, the 15 mT group exhibited the highest survival rate

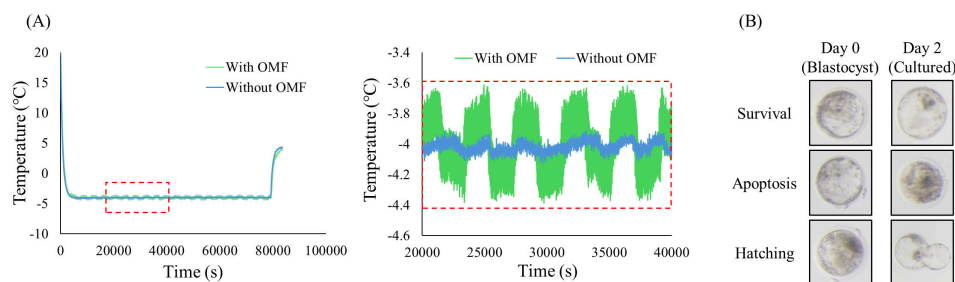


**Fig. 8.** Embryo supercooling preservation results. (A) Temperature profile within the chamber under oscillating magnetic field (OMF) and non-OMF conditions during embryo preservation. (B) Microscopic image showing the typical morphology of embryos surviving and degenerating after supercooling preservation.

**Table 3.** Effects of the magnetic flux density on the survival rate of bovine embryos during supercooling preservation

Magnetic flux density (mT)	No. of embryos	No. of survived (%)
0 (Control)	31	15 ( $48.66 \pm 7.07^a$ )
5	35	21 ( $60.07 \pm 5.48^a$ )
10	35	21 ( $62.85 \pm 5.24^a$ )
15	32	24 ( $75.69 \pm 4.31^b$ )
20	28	19 ( $68.96 \pm 7.62^b$ )

<sup>a,b</sup>Different letters indicate significant differences ( $p < 0.05$ ).

(75.69%  $\pm$  4.31%), whereas the 20 mT group showed a slightly lower rate (68.96%  $\pm$  7.62%). Both the 15 mT and 20 mT groups demonstrated statistically significant differences compared with the control samples ( $p < 0.05$ ).

## DISCUSSION

Previous studies have demonstrated that commonly used hypothermic (2°C–8°C) and cryopreservation (–196°C) approaches still have inherent limitations. In particular, these preservation methods cannot fully prevent cellular injury caused by ice crystal formation, osmotic stress, and cryoprotectant toxicity [21]. Supercooling has emerged as a promising alternative for short- and medium-term preservation, with accumulating evidence supporting its applicability in agricultural and biological materials [22,23]. In this study, we applied supercooling preservation combined with an OMF to maintain the embryos at –4°C without ice formation.

As shown in Fig. 1 and Fig. 2, the Helmholtz-type dual-coil configuration and the double-jacket cooling chamber were designed to minimize coil-induced heating, a factor known to destabilize supercooling environments [24]. Spatial temperature measurements confirmed that the vertical and horizontal variations remained within  $\pm 0.5^\circ\text{C}$  and  $\pm 0.2^\circ\text{C}$ , respectively (Fig. 5, Table 1), indicating that localized warming—which can trigger ice nucleation—was effectively suppressed. Magnetic field measurements also showed high agreement with the simulation results, with discrepancies within  $\pm 5\%$  (Fig. 6), demonstrating that the preservation region received a uniform amount of magnetic flux. Consequently, it was confirmed that the system provided a stable thermal and magnetic environment for evaluating OMF effects.

Before conducting the embryo experiments, we examined whether different magnetic flux densities influenced the cooling behavior of the preservation solution at –4°C. Although magnetic field exposure was expected to stabilize the supercooled state, Fig. 7 shows that the cooling curves were nearly identical across all groups, indicating no measurable effect of the magnetic flux density on the cooling process. Consistent with these results, all samples remained successfully supercooled regardless of the field intensity level (Table 2). These findings suggest that thermodynamic parameters—such as the cooling rate, container geometry, solution composition, and sample volume—play a more dominant role in determining supercooling stability than the magnetic field intensity under the present conditions [19,25,26]. Importantly, the OMF did not induce premature nucleation, contrary to previous reports proposing that an OMF can trigger ice formation [27]. Instead, our data indicates that the OMF posed minimal risk of destabilizing the supercooled state within the tested intensity range. However, given that this study was conducted under a limited range of magnetic field conditions, future studies are needed to investigate the interactions between magnetic field parameters (intensity, frequency, waveform) and temperature on supercooling outcomes more systematically [28].

Blastocyst-stage bovine embryos were preserved in the developed system at –4°C for 24 hours and subsequently cultured for 24 hours to assess viability. As shown in Table 3 and Fig. 8B, survival rates were higher in all magnetic field groups compared with the control group (0 mT), with the highest viability observed at 15 mT (75.69%). The 15 mT group exhibited a statistically significant improvement relative to the controls ( $p < 0.05$ ), whereas a slight decline was observed at 20 mT. The temperature profile during preservation (Fig. 8A) confirmed that embryos experienced stable –4°C conditions throughout the process, indicating that differences in survival were attributable to the magnetic field intensity rather than to thermal fluctuations. Kojima et al. [29] reported that an appropriate combination of the OMF intensity and freezing temperature can modulate intracellular ice formation and dehydration, thereby improving post-thaw cell survival. This principle aligns with

our results, in which viability increased under a specific magnetic field condition. Similarly, studies using static magnetic fields (SMFs) have shown that SMFs can suppress intracellular ice formation and oxidative stress, leading to improved cellular recovery after cryopreservation [30,31]. Although the present study applied an OMF under supercooling rather than freezing conditions, the peak survival observed at 15 mT resembles the stabilizing effects reported for exposure to SMFs, raising the possibility that OMF-induced stabilization effects could involve the modulation of reactive oxygen species (ROS), membrane potential, or mitochondrial function.

In summary, this study demonstrated that exposure to an OMF at  $-4^{\circ}\text{C}$  enhanced embryo survival. This finding stands in contrast to previous reports showing that alternating magnetic fields can exert detrimental effects on mammalian embryos—including increased ROS production, impaired cellular function, morphological abnormalities, and reduced viability [32–34]. Embryo survival increased with the magnetic field intensity up to a certain threshold, beyond which the enhancement plateaued, revealing a nonlinear response. This pattern suggests that a specific magnetic field condition (e.g., 15 mT) may mitigate ROS accumulation or support the maintenance of DNA integrity under low-temperature stress [35]. It is also conceivable that magnetic-field-assisted supercooling influenced the physical state of the intracellular water or the local microenvironment [36]. Meanwhile, magnetic field intensities below 10 mT or above 20 mT showed less pronounced improvements in embryo survival compared to the intermediate field strength settings. Although the observed response may reflect the combined effects of the applied magnetic field parameters, the potential influence of unequal sample sizes and batch-related variability across experimental groups cannot be excluded. Accordingly, these factors should be more rigorously controlled in future studies.

The results of this study demonstrate the feasibility of OMF-assisted supercooling for embryo preservation, indicating that magnetic fields may simultaneously stabilize the supercooled state and support the physiological viability of embryos. However, this study has several limitations. First, only short-term post-preservation viability (1 day) was evaluated; therefore, future studies should assess long-term developmental outcomes ( $\geq 3$  days), including hatching and pregnancy rates. Second, the experiments were conducted under fixed temperature and frequency conditions with a narrow range of magnetic field intensity levels, implying that further research should systematically examine the interactions among temperature conditions and magnetic field parameters (waveform, intensity, frequency). Finally, while several potential biological mechanisms may be hypothesized to explain the observed effects of OMF exposure, these were not directly examined in the present study. Therefore, future studies should directly assess molecular and cellular indicators—such as ROS levels, the membrane potential,  $\text{Ca}^{2+}$  dynamics, and the mitochondrial membrane potential ( $\Delta\Psi\text{m}$ )—to validate these hypotheses.

## CONCLUSION

In this study, we developed and evaluated an OMF-assisted supercooling system for the preservation of bovine IVF embryos at  $-4^{\circ}\text{C}$ . The combined use of Helmholtz coils and a circulation-based cooling system ensured uniform thermal and magnetic field stability, and no freezing occurred under any condition. Embryo survival was significantly improved at 15 mT compared with the control group, indicating that magnetic fields may enhance cellular stability within a specific intensity range during supercooling preservation.

In contrast, no thermodynamic differences were detected in the preservation solution, suggesting that factors such as the cooling rate and container geometry exert stronger control over supercooling behavior than magnetic field exposure. Future studies should quantitatively assess the interactions

among magnetic field parameters and temperature conditions and further evaluate long-term developmental outcomes, including hatching and pregnancy rates.

Collectively, these findings demonstrate that an OMF can simultaneously suppress freezing and improve embryo survival during supercooling, providing a foundational basis for magnetic-field-based, non-freezing preservation strategies for biological specimens.

## REFERENCES

1. Sirard MA. 40 years of bovine IVF in the new genomic selection context. *Reproduction*. 2018;156:R1-7. <https://doi.org/10.1530/REP-18-0008>
2. Huang Z, Gao L, Hou Y, Zhu S, Fu X. Cryopreservation of farm animal gametes and embryos: recent updates and progress. *Front Agr Sci Eng*. 2019;6:42-53. <https://doi.org/10.15302/J-FASE-2018231>
3. Valente RS, Marsico TV, Sudano MJ. Basic and applied features in the cryopreservation progress of bovine embryos. *Anim Reprod Sci*. 2022;239:106970. <https://doi.org/10.1016/j.anireprosci.2022.106970>
4. Marqui FN, Martins A Jr, Cardoso TC, Cruz TE, Dell'Aqua JA Jr, Oba E. Cooling of in vitro-produced bovine embryos: effects of medium and time on gene expression, DNA fragmentation and embryonic survival. *Livest Sci*. 2019;230:103811. <https://doi.org/10.1016/j.livsci.2019.09.027>
5. Fuller BJ, Petrenko AY, Rodriguez JV, Somov AY, Balaban CL, Guibert EE. Biopreservation of hepatocytes: current concepts on hypothermic preservation, cryopreservation, and vitrification. *Cryoletters*. 2013;37:432-52.
6. Ideta A, Aoyagi Y, Tsuchiya K, Kamijima T, Nishimiya Y, Tsuda S. A simple medium enables bovine embryos to be held for seven days at 4 °C. *Sci Rep*. 2013;3:1173. <https://doi.org/10.1038/srep01173>
7. Ideta A, Aoyagi Y, Tsuchiya K, Nakamura Y, Hayama K, Shirasawa A, et al. Prolonging hypothermic storage (4 C) of bovine embryos with fish antifreeze protein. *J Reprod Dev*. 2015;61:1-6. <https://doi.org/10.1262/jrd.2014-073>
8. Murray KA, Gao Y, Griffiths CA, Kinney NLH, Guo Q, Gibson MI, et al. Chemically induced extracellular ice nucleation reduces intracellular ice formation enabling 2D and 3D cellular cryopreservation. *JACS Au*. 2023;3:1314-20. <https://doi.org/10.1021/jacsau.3c00056>
9. Preciado J, Rubinsky B. The effect of isochoric freezing on mammalian cells in an extracellular phosphate buffered solution. *Cryobiology*. 2018;82:155-8. <https://doi.org/10.1016/j.cryobiol.2018.04.004>
10. Usta OB, Kim Y, Ozer S, Bruinsma BG, Lee J, Demir E, et al. Supercooling as a viable non-freezing cell preservation method of rat hepatocytes. *PLOS ONE*. 2013;8:e69334. <https://doi.org/10.1371/journal.pone.0069334>
11. William N, Isiksacan Z, Mykhailova O, Olafson C, Yarmush ML, Usta OB, et al. Comparing two extracellular additives to facilitate extended storage of red blood cells in a supercooled state. *Front Physiol*. 2023;14:1165330. <https://doi.org/10.3389/fphys.2023.1165330>
12. Hikichi M, Shimizu T, Sato K. Development of supercooling preservation method of adherent cultured human cells. *J Biochem*. 2023;174:273-8. <https://doi.org/10.1093/jb/mvad040>
13. Huang H, Yarmush ML, Usta OB. Long-term deep-supercooling of large-volume water and red cell suspensions via surface sealing with immiscible liquids. *Nat Commun*. 2018;9:3201. <https://doi.org/10.1038/s41467-018-05636-0>
14. Gholami D, Ghaffari SM, Riazi G, Fathi R, Benson J, Shahverdi A, et al. Electromagnetic

- field in human sperm cryopreservation improves fertilizing potential of thawed sperm through physicochemical modification of water molecules in freezing medium. *PLOS ONE*. 2019;14:e0221976. <https://doi.org/10.1371/journal.pone.0221976>
15. Gou Y, Qin Y, Li J, Zhang W, Liu J, Wang Z. Effect of a magnetic field on droplet freezing and frost formation on cold surfaces. *Cryobiology*. 2024;114:104866. <https://doi.org/10.1016/j.cryobiol.2024.104866>
  16. Jun S, Ko Y, Lee SH. Explorative supercooling technology for prevention of freeze damages in vaccines. *Appl Sci*. 2022;12:3173. <https://doi.org/10.3390/app12063173>
  17. Kong F, Li P, Zhang H, Tian C, Leng D, Hou C. Enhanced supercooling of water with a 6 mT/50 Hz oscillating magnetic field and its application in fruit preservation. *Food Bioprocess Technol*. 2024;17:4239-48. <https://doi.org/10.1007/s11947-024-03384-2>
  18. Ju BH, Kim YJ, Park YB, Kim BH, Kim MK. Evaluation of conical 9 well dish on bovine oocyte maturation and subsequent embryonic development. *J Anim Sci Technol*. 2024;66:936-48. <https://doi.org/10.5187/jast.2024.e68>
  19. Kang T, Hoptowit R, Jun S. Effects of an oscillating magnetic field on ice nucleation in aqueous iron-oxide nanoparticle dispersions during supercooling and preservation of beef as a food application. *J Food Process Eng*. 2020;43:e13525. <https://doi.org/10.1111/jfpe.13525>
  20. Beguš S, Bojkovski J, Drnovšek J, Geršak G. Magnetic effects on thermocouples. *Meas Sci Technol*. 2014;25:035006. <https://doi.org/10.1088/0957-0233/25/3/035006>
  21. Elliott GD, Wang S, Fuller BJ. Cryoprotectants: a review of the actions and applications of cryoprotective solutes that modulate cell recovery from ultra-low temperatures. *Cryobiology*. 2017;76:74-91. <https://doi.org/10.1016/j.cryobiol.2017.04.004>
  22. Jiang H, Hong W, Zhang Y, Liu S, Jiang H, Xia S, et al. Effects of static magnetic field-prolonged supercooling preservation on blueberry quality. *Food Biosci*. 2024;59:103771. <https://doi.org/10.1016/j.fbio.2024.103771>
  23. Lee DY, You YS, Ho KKH, Li Y, Jun SJ. Impact of supercooling storage on physical and chemical properties of yellowfin tuna (*Thunnus albacares*). *J Food Eng*. 2024;373:111818. <https://doi.org/10.1016/j.jfoodeng.2023.111818>
  24. Kang T, You YS, Hoptowit R, Wall MM, Jun S. Effect of an oscillating magnetic field on the inhibition of ice nucleation and its application for supercooling preservation of fresh-cut mango slices. *J Food Eng*. 2021;300:110541. <https://doi.org/10.1016/j.jfoodeng.2021.110541>
  25. Otero L, Rodríguez AC, Pérez-Mateos M, Sanz PD. Effects of magnetic fields on freezing: application to biological products. *Compr Rev Food Sci Food Saf*. 2016;15:646-67. <https://doi.org/10.1111/1541-4337.12202>
  26. John Morris G, Acton E. Controlled ice nucleation in cryopreservation – a review. *Cryobiology*. 2013;66:85-92. <https://doi.org/10.1016/j.cryobiol.2012.11.007>
  27. Ruan J, Wang H, Zhao J, Li D, Yang H. Effect of magnetic field on frozen food quality characteristics. *Food Eng Rev*. 2024;16:396-421. <https://doi.org/10.1007/s12393-024-09366-6>
  28. Rodríguez AC, Otero L, Cobos JA, Sanz PD. Electromagnetic freezing in a widespread frequency range of alternating magnetic fields. *Food Eng Rev*. 2019;11:93-103. <https://doi.org/10.1007/s12393-019-09190-3>
  29. Kojima S, Kaku M, Kawata T, Sumi H, Shikata H, Abonti TR, et al. Cryopreservation of rat MSCs by use of a programmed freezer with magnetic field. *Cryobiology*. 2013;67:258-63. <https://doi.org/10.1016/j.cryobiol.2013.08.003>
  30. Baniyasi F, Hajiaghajlou S, Shahverdi A, Ghalebaboran MR, Pirhajati V, Fathi R. The beneficial effects of static magnetic field and iron oxide nanoparticles on the vitrification of mature mice oocytes. *Reprod Sci*. 2023;30:2122-36. <https://doi.org/10.1007/s43032-022-01144-1>

31. Baniasadi F, Hajiaghalou S, Shahverdi A, Pirhajati V, Fathi R. Static magnetic field halves cryoinjuries of vitrified mouse COCs, improves their functions and modulates pluripotency of derived blastocysts. *Theriogenology*. 2021;163:31-42. <https://doi.org/10.1016/j.theriogenology.2020.12.025>
32. Zadeh-Haghighi H, Simon C. Magnetic field effects in biology from the perspective of the radical pair mechanism. *J R Soc Interface*. 2022;19:20220325. <https://doi.org/10.1098/rsif.2022.0325>
33. Chen JS, Tsai LK, Yeh TY, Li TS, Li CH, Wei ZH, et al. Effects of electromagnetic waves on oocyte maturation and embryonic development in pigs. *J Reprod Dev*. 2021;67:392-401. <https://doi.org/10.1262/jrd.2021-074>
34. Seify M, Khalili MA, Anbari F, Koohestanidehaghi Y. Detrimental effects of electromagnetic radiation emitted from cell phone on embryo morphokinetics and blastocyst viability in mice. *Zygote*. 2024;32:149-53. <https://doi.org/10.1017/S0967199424000042>
35. Dahr NK, Abdolmaleki P, Halvaei I. Static magnetic field can ameliorate detrimental effects of cryopreservation on human spermatozoa. *Rev Int Androl*. 2024;22:27-34. <https://doi.org/10.22514/j.androl.2024.012>
36. Okuda K, Kaori K, Kawauchi A, Miyu I, Yomogida K. An oscillating magnetic field suppresses ice-crystal growth during rapid freezing of muscle tissue of mice. *J Biochem*. 2023;175:mvad087. <https://doi.org/10.1093/jb/mvad087>